Open Access

Earth System
Science
Data

Discussions

Discussion Paper | Discussion Paper | Discussion Paper | Discussion Paper

ESSDD

6, 367–388, 2013

**Trace elements at Cape Verde**

R. Sander et al.

Title Page

Abstract | Instruments

Data Provenance & Structure

Tables | Figures

|◄ | ►|

◄ | ►

Back | Close

Full Screen / Esc

Printer-friendly Version

Interactive Discussion

# Gas phase acid, ammonia and aerosol ionic and trace element concentrations at Cape Verde during the Reactive Halogens in the Marine Boundary Layer (RHaMBLe) 2007 intensive sampling period

R. Sander[1], A. A. P. Pszenny[2], W. C. Keene[3], E. Crete[2,*], B. Deegan[4,**], M. S. Long[3,***], J. R. Maben[3], and A. H. Young[2]

[1]Air Chemistry Department, Max-Planck Institute of Chemistry, P.O. Box 3060, 55020 Mainz, Germany
[2]University of New Hampshire, Durham, USA
[3]Department of Environmental Sciences, University of Virginia, Charlottesville, VA 22904, USA
[4]Mount Washington Observatory, North Conway, New Hampshire, USA
[*]now at: The Earth Institute, Columbia University, NY, USA
[**]now at: 97 Raymond St., Fairhaven, MA, USA
[***]now at: Harvard University, Cambridge, MA

Title Page

Abstract | Instruments

Data Provenance & Structure

Tables | Figures

◄ | ►|

◄ | ►

Back | Close

Full Screen / Esc

Printer-friendly Version

Interactive Discussion

## Abstract

We report mixing ratios of soluble reactive trace gases sampled with mist chambers and the chemical composition of bulk aerosol and volatile inorganic bromine ($Br_g$) sampled with filter packs during the Reactive Halogens in the Marine Boundary Layer (RHaMBLe) field campaign at the Cape Verde Atmospheric Observatory (CVAO) on São Vicente island in the tropical North Atlantic in May and June 2007. The gas-phase data include $HCl$, $HNO_3$, $HONO$, $HCOOH$, $CH_3COOH$, $NH_3$, and volatile reactive chlorine other than $HCl$ ($Cl^*$). Aerosol samples were analyzed by neutron activation (Na, Al, Cl, V, Mn, and Br) and ion chromatography ($SO_4^{2-}$, $Cl^-$, $Br^-$, $NH_4^+$, $Na^+$, $K^+$, $Mg^{2+}$, and $Ca^{2+}$). Content and quality of the data, which are available under doi:10.5281/zenodo.6956, are presented and discussed.

## 1 Introduction

Multiphase halogen chemistry impacts important, interrelated chemical processes in marine air. Bromine activation chemistry leads to catalytic ozone destruction and modification of oxidation processes including $HO_x$ and $NO_x$ cycling. Spatiotemporal variability in many reactants, products and reaction pathways are poorly characterized, rendering uncertain the global significance of tropospheric halogen chemistry.

## 2 Dataset description and access

During the RHaMBLe campaign in spring 2007 (Lee et al., 2010), we measured constituents of marine air from a 30 m-tall sampling tower (Fig. 1) at the Cape Verde Atmospheric Observatory on the windward shore of São Vicente Island (16.8° N, 24.9° W, see Fig. 2). The data are available under doi:10.5281/zenodo.6956.

# 3 Instruments and methods

All air volumes reported here are normalized to standard temperature and pressure (273 K and $1.013 \times 10^5$ Pa).

## 3.1 Mist chambers

Water-soluble, volatile inorganic chlorine and nitrate (dominated by and hereafter referred to as HCl and $HNO_3$, respectively), $NH_3$, HCOOH, and $CH_3COOH$ were sampled over 2 h intervals at nominal flow rates of 20 L min$^{-1}$ with a single set of tandem mist chambers (Figs. 3 and 4), each of which contained 20 ml deionized water (Lawler et al., 2009). To minimize artifact phase changes caused by mixing chemically distinct aerosol size fractions on bulk prefilters, air was sampled through a size-fractionating inlet that inertially removed super-µm aerosols from the sample stream. Sub-µm aerosol was removed downstream by an in-line 47 mm Teflon filter (Zefluor 2 µm pore diameter). In-line filters were changed daily. Samples were analyzed on site by ion chromatography (IC) usually within a few hours after recovery. Data were corrected based on dynamic handling blanks that were loaded, briefly (few seconds) exposed to ambient air flow, recovered, processed, and analyzed using procedures identical to those for samples. Collection efficiencies for all species were greater than 95 % and, consequently, corrections for inefficient sampling were not necessary. Relative precisions based on paired measurements varied as functions of concentration and typically averaged ±10 % to ±25 %. Average detection limits (DLs; estimated following Keene et al., 1989) for HCl, $HNO_3$, $NH_3$, HCOOH, and $CH_3COOH$ were 26, 12, 3, 29, and 44 pmol mol$^{-1}$, respectively.

Reactive inorganic chlorine gases (Cl$^*$) were sampled in parallel through an identical inlet with similar set of tandem mist chambers samplers (Keene et al., 1993; Maben et al., 1995; Lawler et al., 2009). The upstream chamber contained acidic solution (37.5 mM $H_2SO_4$ and 0.042 mM $(NH_4)_2SO_4$), which removed HCl quantitatively but efficiently passed other forms of volatile Cl, and the downstream chamber contained

alkaline solution (30.0 mM NaHCO$_3$ and 0.408 mM NaHSO$_3$), which sampled Cl* (including Cl$_2$ HOCl, and probably contributions from ClNO$_3$, ClNO$_2$, BrCl, ClO, and Cl). Available evidence (Keene et al., 1993; Maben et al., 1995) indicates that this sampling technique reliably discriminates volatile inorganic Cl from Cl associated with both

5 particles and organic gases and that it quantitatively differentiates between HCl and other forms of volatile inorganic Cl. However, the speciation of Cl* cannot be determined unequivocally. Mist solutions were analyzed on site by IC. The average precision for Cl* was approximately $\pm 15\%$ or $\pm 7$ pmol mol$^{-1}$ Cl, whichever was the greater absolute value, and the corresponding average DL based on Keene et al. (1989) was

10 14 pmol mol$^{-1}$ Cl.

## 3.2 Filter-pack sampling and chemical analysis

Using a modification of the technique by Rahn et al. (1976), total aerosol and inorganic gases were sampled using filter packs with 3 filters (Fig. 5). Particles were sampled on dry 47 mm diameter Whatman 41 cellulose filters that were positioned upstream

15 (W1 in Fig. 5). Each filter was precleaned with deionized water (DIW) and dried prior to the campaign. Alkaline-reactive trace gases were sampled on moist tandem Rayon filters (SKU 64007, Leader Evaporator), impregnated with an alkaline solution (10 g LiOH and 10 mL glycerol per 100 mL), positioned in tandem downstream (R1 and R2 in Fig. 5). Filters from the same lot were used for all samples, blanks, and analyti-

20 cal standards. Sample and field blank filters were mounted in 47 mm diameter Nuclepore polycarbonate cassettes. Seven samples were collected each day with sample changes keyed to sunrise and sunset and other change times adjusted such that sampling interval durations were similar (3 to 4 h). The airflow was about 80 standard liters per minute (SLPM) and monitored with a mass flow meter. Field blanks were obtained

25 once per day at different times. Each field blank was loaded, deployed, exposed briefly (few seconds) to ambient air, recovered, processed, and analyzed using procedures identical to those for samples. Between each use filter cassettes were completely disassembled, cleaned with dilute Liquinox solution, rinsed with DIW and dried in a clean

bench. Exposed filters were transferred to clean polyethylene envelopes, frozen, and transported to and stored frozen at the University of New Hampshire (UNH) prior to preparation for analysis.

Using tandem impregnated filters allowed to calculate the collection efficiency $\varepsilon$ for volatile inorganic bromine $Br_g$:

$$\varepsilon = \frac{m_1}{m_{tot}} = \frac{m_2}{(m_{tot} - m_1)} \tag{1}$$

Here, $m_1$ and $m_2$ are the masses deposited on the first and second impregnated filter, respectively, and $m_{tot}$ is the total mass that would be deposited at 100 % collection efficiency. Rearranging the equations and inserting the known values of $m_1$ and $m_2$ yields a collection efficiency of

$$\varepsilon = 1 - m_2/m_1 \tag{2}$$

and a total mass of

$$m_{tot} = \frac{m_1}{1 - m_2/m_1} \tag{3}$$

All filters were analyzed by neutron activation analysis (NAA) using a procedure based on that described by Uematsu et al. (1983). Standards were prepared by spotting aliquots of a NIST-traceable mixed element standard solution (Ultra Scientific, North Kingstown, RI) on blank filter circles. Standards, samples and field blanks were each spiked with 20 ng of indium in dilute nitric acid (as an aliquot of a NIST-traceable standard solution; Ultra Scientific) as internal flux monitor, sealed in a clean polyethylene envelope and subsequently irradiated at the Rhode Island Nuclear Science Center (RINSC) for 300 s at a nominal flux of $4 \times 10^{12} \, cm^{-2} \, s^{-1}$ thermal neutrons. Following irradiation, samples were allowed to decay for approximately 5 min during which they were transferred to non-irradiated envelopes, and counted for 900 s live time on a

Ge(Li) gamma-ray spectrometer. From the particle filters, data were obtained for six elements: Na, Al, Cl, Mn, V, and Br. Using Eq. (3), gaseous Br data were obtained from the impregnated filters. All laboratory manipulations of cassettes and filters prior to irradiation were carried out in class 100 clean benches by personnel wearing unpowdered plastic gloves.

About three years after the NAA analysis, the radioactivity had decreased to a safe level, and it was possible to handle the samples again. The aerosols on the particle filters were extracted under sonication in DIW. The ionic species $SO_4^{2-}$, $Cl^-$, $Br^-$, $NH_4^+$, $Na^+$, $K^+$, $Mg^{2+}$, and $Ca^{2+}$ were determined by high-performance ion chromatography (IC) using procedures similar to those described by Keene et al. (2009). Data for samples were corrected based on median concentrations of analytes recovered from handling blanks ($n = 10$).

To estimate the detection limits for the filter pack aerosol samples, we used Eq. (14) of Currie (1995). An element or ion was deemed detected if its mass (NAA) or extract concentration (IC) exceeded its minimal detectable value estimated via:

$$DL = 2\,t_{1-\alpha,\nu}\,s_0 \tag{4}$$

where DL is the detection limit (minimal detectable value), $t$ is the value of Student's $t$ statistic for probability level $\alpha$ and $\nu$ degrees of freedom (= number of blanks), and $s_0$ is the standard deviation of mass or concentration values determined in the $N$ blanks analyzed. The choice of $\alpha = 0.025$ corresponds to rejecting a null hypothesis of "not detected" at the 95 % confidence level. The average sampled air volume for all samples of 12.4 m$^3$ STP (0 °C, 1 atm) was assumed for all calculations.

For IC, the blanks' analyses indicated two distinct subsets of blanks of $N = 3$ and $N = 20$, respectively, with quite different concentrations of several ions. For NAA, chlorine appeared to have the same two subsets. For other elements determined no distinct subsets were apparent.

The phase partitioning of HCl and $NH_3$ with aerosol solutions is pH dependent, and aerosol pH typically varies as a function of size. Because the pH of aerosols sampled

in bulk on a filter may diverge from the pH of the aerosol size fractions with which most $Cl^-$ and $NH_4^+$ is associated in ambient air, these species are subject to artifact phase changes when sampled in bulk (e.g., Keene et al., 1990). Consequently, the absolute concentrations and associated enrichment factors and deficits relative to sea salt that are reported herein may not be representative of those for ambient aerosols during the campaign.

## 4  Data summary

A detailed analysis of the measurement data is beyond the scope of this paper. Here we only want to present some basic results and show some plots for quality assurance. Minimum, maximum, average, and median values are shown in Table 1. Adopting the equations from Sander et al. (2003) and using the seawater mass ratios $([Cl]/[Na])_{seawater} = 1.8\,\mathrm{kg\,kg^{-1}}$ and $([Br]/[Na])_{seawater} = 0.0062\,\mathrm{kg\,kg^{-1}}$, we define the enrichment factors EF(X) for X = Cl and Br as:

$$EF(X) = \frac{[X]/[Na]}{([X]/[Na])_{seawater}} \qquad (5)$$

where square brackets denote mass concentrations. Another useful quantity is the absolute deficit, which is defined as:

$$\text{deficit} = \left[ [Na] \times \left( \frac{[X]}{[Na]} \right)_{seawater} \right] - [X] \qquad (6)$$

We also define the quantity ΔBr, which is the difference between gas-phase bromine and the bromine deficit.

- Time series of the mist chamber data are shown in Fig. 6.
- Time series of the filter pack data (NAA) are shown in Fig. 7.

374

– Time series of the filter pack data (IC) are shown in Fig. 8.

– Scatter plots of paired data for selected analytes are shown in Fig. 10.

– The presence of volatile acids at detectable mixing ratios indicates that aerosols were either acidic or rapidly acidified throughout the campaign.

– The very good correlations between Na and Cl measured by NAA vs IC (Fig. 10) coupled with slopes and intercepts that are statistically indistinguishable from 1.0 and 0.0, respectively, indicate that (1) virtually all particulate Na and Cl were in the forms $Na^+$ and $Cl^-$, respectively, and (2) $Na^+$ and $Cl^-$ in samples did not deteriorate while stored for 3 yr.

– EF(Br) was not correlated with particulate $Na^+$. Absolute deficits of particulate Br and mixing ratios of gas-phase bromine ($Br_g$) increased with increasing sea-salt concentrations. These relationships together with the presence of acidic gases at detectable levels indicate that sufficient acidity was available to titrate sea-salt alkalinity and sustain halogen activation over the full range of sea-salt loadings during the experiment.

– $Br_g$ concentrations are almost always higher than absolute deficits of particulate Br (the difference is shown as "delta Br" in Fig. 7). This implies that $Br_g$ has a longer atmospheric lifetime than the parent aerosol. This has also been observed in a previous campaign (Keene et al., 2009).

– Good correlation between Al and Mn (Fig. 10) indicates a common origin (crustal dust).

– Good correlation between HCOOH and $CH_3COOH$ (Fig. 10) suggests common sources and/or processing.

– Systematic diel variability was evident in neither aerosol Br enrichment factor nor inorganic gaseous Br (Fig. 9). This is in contrast to previous measurements in the

MBL at Hawaii (Sander et al., 2003) and over the eastern Atlantic (Keene et al., 2009).

# References

10  Currie, L. A.: Nomenclature in evaluation of analytical methods including detection and quantification capabilities, Pure Appl. Chem., 67, 1699–1723, 1995. 373

Keene, W. C., Talbot, R. W., Andreae, M. O., Beecher, K., Berresheim, H., Castro, M., Farmer, J. C., Galloway, J. N., Hoffmann, M. R., Li, S.-M., Maben, J. R., Munger, J. W., Norton, R. B., Pszenny, A. A. P., Puxbaum, H., Westberg, H., and Winiwarter, W.: An intercomparison of

15  measurement systems for vapor and particulate phase concentrations of formic and acetic acids, J. Geophys. Res., 94D, 6457–6471, 1989. 370, 371

Keene, W. C., Pszenny, A. A. P., Jacob, D. J., Duce, R. A., Galloway, J. N., Schultz-Tokos, J. J., Sievering, H., and Boatman, J. F.: The geochemical cycle of reactive chlorine through the marine troposphere, Global Biogeochem. Cycles, 4, 407–430, 1990. 374

20  Keene, W. C., Maben, J. R., Pszenny, A., and Galloway, J. N.: Measurement technique for inorganic chlorine gases in the marine boundary layer, Environ. Sci. Technol., 27, 866–874, 1993. 370, 371

Keene, W. C., Long, M. S., Pszenny, A. A. P., Sander, R., Maben, J. R., Wall, A. J., O'Halloran, T. L., Kerkweg, A., Fischer, E. V., and Schrems, O.: Latitudinal variation in the multiphase

25  chemical processing of inorganic halogens and related species over the eastern North and South Atlantic Oceans, Atmos. Chem. Phys., 9, 7361–7385, doi:10.5194/acp-9-7361-2009, 2009. 373, 375, 376

Lawler, M. J., Finley, B. D., Keene, W. C., Pszenny, A. A. P., Read, K. A., von Glasow, R., and Saltzman, E. S.: Pollution-enhanced reactive chlorine chemistry in the eastern tropical

Title Page

Abstract | Instruments

Data Provenance & Structure

Tables | Figures

◄◄ | ►►

◄ | ►

Back | Close

Full Screen / Esc

Printer-friendly Version

Interactive Discussion

Atlantic boundary layer, Geophys. Res. Lett., 36, L08810, doi:10.1029/2008GL036666, 2009. 370

Lee, J. D., McFiggans, G., Allan, J. D., Baker, A. R., Ball, S. M., Benton, A. K., Carpenter, L. J., Commane, R., Finley, B. D., Evans, M., Fuentes, E., Furneaux, K., Goddard, A., Good, N., Hamilton, J. F., Heard, D. E., Herrmann, H., Hollingsworth, A., Hopkins, J. R., Ingham, T., Irwin, M., Jones, C. E., Jones, R. L., Keene, W. C., Lawler, M. J., Lehmann, S., Lewis, A. C., Long, M. S., Mahajan, A., Methven, J., Moller, S. J., Müller, K., Müller, T., Niedermeier, N., O'Doherty, S., Oetjen, H., Plane, J. M. C., Pszenny, A. A. P., Read, K. A., Saiz-Lopez, A., Saltzman, E. S., Sander, R., von Glasow, R., Whalley, L., Wiedensohler, A., and Young, D.: Reactive Halogens in the Marine Boundary Layer (RHaMBLe): the tropical North Atlantic experiments, Atmos. Chem. Phys., 10, 1031–1055, doi:10.5194/acp-10-1031-2010, 2010. 369

Maben, J. R., Keene, W. C., Pszenny, A. A. P., and Galloway, J. N.: Volatile inorganic Cl in surface air over eastern North America, Geophys. Res. Lett., 22, 3513–3516, 1995. 370, 371

Rahn, K. A., Borys, R. D., and Duce, R. A.: Tropospheric halogen gases: Inorganic and organic components, Science, 192, 549–550, 1976. 371

Sander, R., Keene, W. C., Pszenny, A. A. P., Arimoto, R., Ayers, G. P., Baboukas, E., Cainey, J. M., Crutzen, P. J., Duce, R. A., Hönninger, G., Huebert, B. J., Maenhaut, W., Mihalopoulos, N., Turekian, V. C., and Van Dingenen, R.: Inorganic bromine in the marine boundary layer: a critical review, Atmos. Chem. Phys., 3, 1301–1336, doi:10.5194/acp-3-1301-2003, 2003. 374, 376

Uematsu, M., Duce, R. A., Prospero, J. M., Chen, L., Merrill, J. T., and McDonald, R. L.: Transport of mineral aerosol from Asia over the North Pacific Ocean, J. Geophys. Res., 88C, 5343–5352, 1983. 372

Title Page

Abstract | Instruments

Data Provenance & Structure

Tables | Figures

|◀ | ▶|

◀ | ▶

Back | Close

Full Screen / Esc

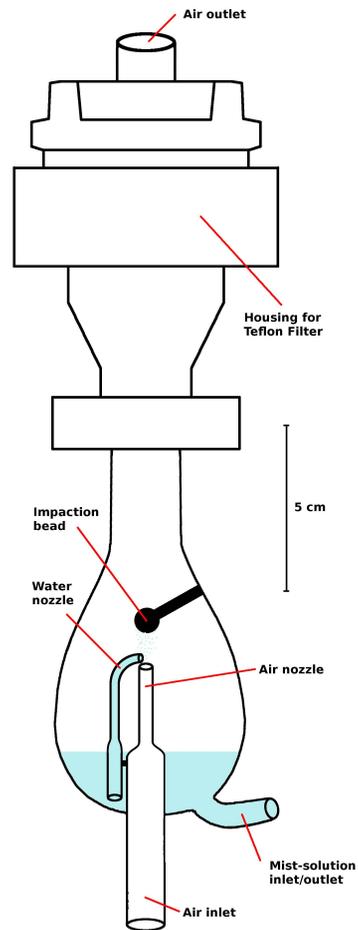Printer-friendly Version

Interactive Discussion

**Table 1.** Data summary. Here, DL is the detection limit. $N(\text{tot})$ and $N (< \text{DL})$ are the total number of data points and the number below the DL, respectively.

| | minimum | maximum | median | DL[*] | $N(\text{tot})$ | $N (< \text{DL})$ | unit |
|---|---|---|---|---|---|---|---|
| | | | | mist chamber | | | |
| HCl | <DL | 613 | 206 | 26 | 212 | 13 | $\text{pmol mol}^{-1}$ |
| Cl[*] | <DL | 222 | 21 | 14 | 212 | 79 | $\text{pmol mol}^{-1}$ |
| $HNO_3$ | <DL | 124 | 14 | 12 | 212 | 90 | $\text{pmol mol}^{-1}$ |
| $NH_3$ | <DL | 651 | 18 | 3 | 212 | 51 | $\text{pmol mol}^{-1}$ |
| HCOOH | <DL | 796 | 128 | 29 | 212 | 68 | $\text{pmol mol}^{-1}$ |
| $CH_3COOH$ | <DL | 550 | 78 | 44 | 212 | 68 | $\text{pmol mol}^{-1}$ |
| | | | | filter pack (NAA) | | | |
| Na | 1.12 | 7.69 | 3.3 | 0.031 | 147 | 0 | $\mu\text{g m}^{-3}$ |
| Al | <DL | 0.559 | 0.095 | 0.013 | 147 | 2 | $\mu\text{g m}^{-3}$ |
| Cl | 0.39 | 6.84 | 2.6 | 0.079, 0.13 | 147 | 0 | $\mu\text{g m}^{-3}$ |
| EF(Cl) | 0.194 | 0.752 | 0.432 | | 147 | | |
| Cl deficit | 1.21 | 6.96 | 3.17 | | 147 | | $\mu\text{g m}^{-3}$ |
| V | <DL | 2.21 | 0.68 | 0.26 | 147 | 16 | $\text{ng m}^{-3}$ |
| Mn | <DL | 4.98 | 1.12 | 0.52 | 147 | 17 | $\text{ng m}^{-3}$ |
| Br | <DL | 26.3 | 8.39 | 4.2 | 147 | 35 | $\text{ng m}^{-3}$ |
| EF(Br) | 0.0524 | 1.06 | 0.392 | | 147 | | |
| Br deficit | −1.33 | 36.7 | 11.3 | | 147 | | $\text{ng m}^{-3}$ |
| $Br_g$ | 3.26 | 41.7 | 16.8 | | 147 | | $\text{ng m}^{-3}$ |
| ΔBr | −20.8 | 29.2 | 5.48 | | 147 | | $\text{ng m}^{-3}$ |
| | | | | filter pack (IC) | | | |
| $Cl^-$ | 0.168 | 7.66 | 2.65 | 0.14, 0.2 | 147 | 1 | $\mu\text{g m}^{-3}$ |
| $EF(Cl^-)$ | 0.0723 | 0.763 | 0.447 | | 147 | | |
| $Cl^-$ deficit | 1.31 | 6.53 | 2.96 | | 147 | | $\mu\text{g m}^{-3}$ |
| $Br^-$ | <DL | 16.7 | 4.59 | 1.3, 8.2 | 147 | 115 | $\text{ng m}^{-3}$ |
| $EF(Br^-)$ | 0.0605 | 0.963 | 0.227 | | 147 | | |
| $Br^-$ deficit | 0.404 | 40.2 | 14.3 | | 147 | | $\text{ng m}^{-3}$ |
| $SO_4^{2-}$ | 0.866 | 6.26 | 2.36 | 0.09, 0.036 | 147 | 0 | $\mu\text{g m}^{-3}$ |
| $Na^+$ | 1.11 | 7.91 | 3.2 | 0.069, 0.14 | 147 | 0 | $\mu\text{g m}^{-3}$ |
| $NH_4^+$ | <DL | 1.11 | 0.292 | 0.49, 0.19 | 147 | 51 | $\mu\text{g m}^{-3}$ |
| $K^+$ | <DL | 0.31 | 0.146 | 0.064, 0.11 | 147 | 32 | $\mu\text{g m}^{-3}$ |
| $Mg^{2+}$ | 0.143 | 0.979 | 0.418 | 0.046, 0.006 | 147 | 0 | $\mu\text{g m}^{-3}$ |
| $Ca^{2+}$ | <DL | 0.632 | 0.19 | 0.35, 0.15 | 147 | 59 | $\mu\text{g m}^{-3}$ |

[*] For IC and for chloride from NAA, the blanks' analyses indicated two distinct subsets with quite different concentrations of several ions. Individual detection limits were calculated for these subsets.

**Trace elements at Cape Verde**

R. Sander et al.

**Fig. 1.** The sampling tower at the Cape Verde Atmospheric Observatory.
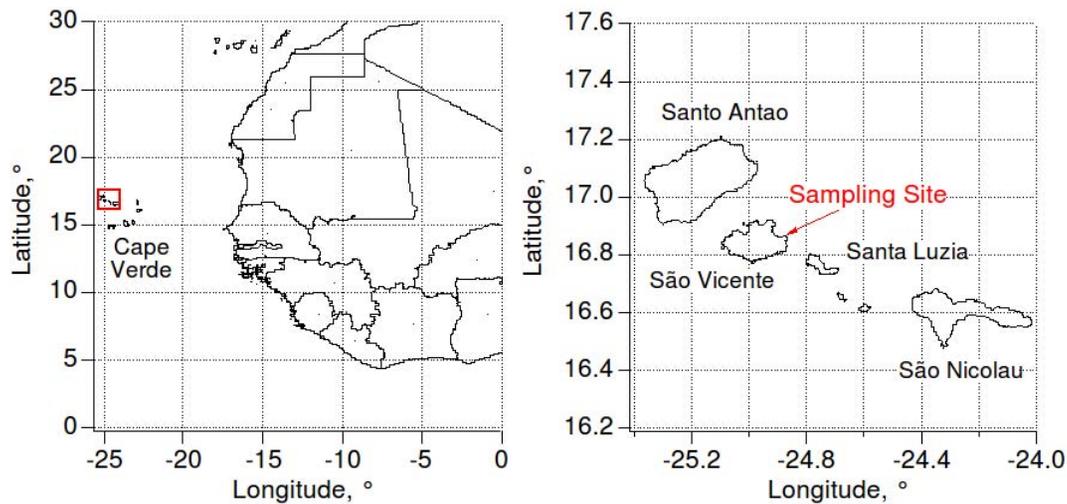
**Fig. 2.** Location of the sampling site.

**Fig. 3.** Mist chambers at the Cape Verde sampling tower.

Title Page

Abstract | Instruments

Data Provenance & Structure

Tables | Figures

Back | Close

Full Screen / Esc

Printer-friendly Version

Interactive Discussion

Air outlet

Housing for
Teflon Filter

5 cm

Impaction
bead

Water
nozzle

Air nozzle

Mist-solution
inlet/outlet

Air inlet

**Fig. 4.** Schematic of a mist chamber (to scale). The teflon filter (only housing is shown) serves as a liquid barrier.
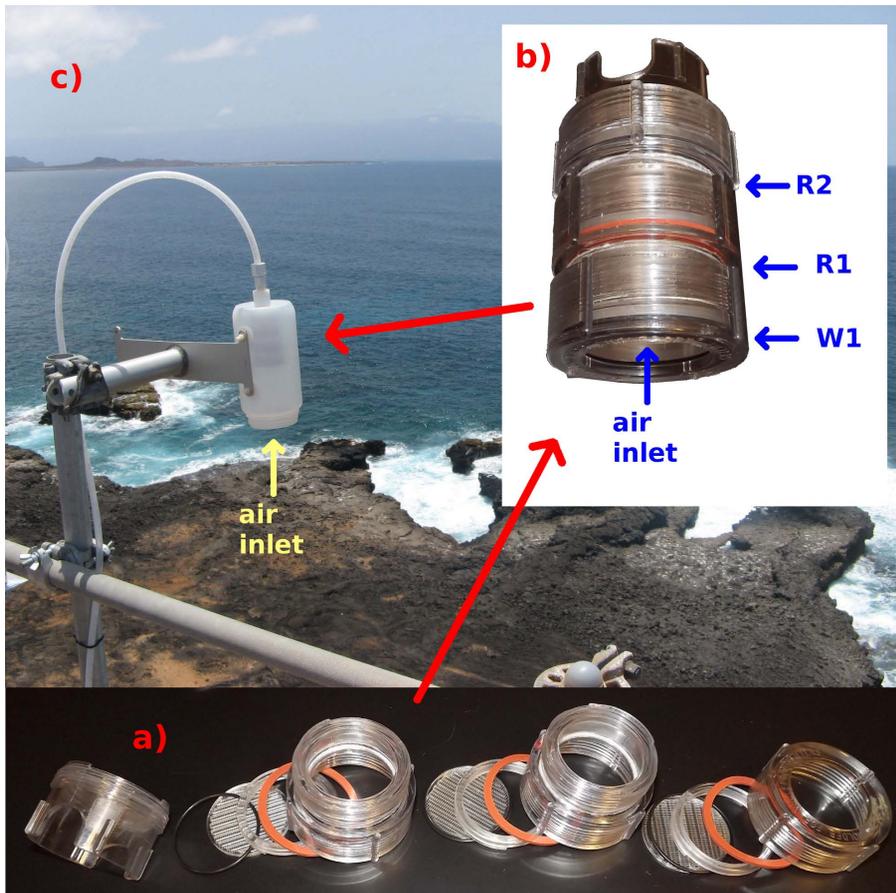
**Fig. 5.** Filter packs: **(a)** individual pieces (without filters); **(b)** assembled filter pack with positions of the Whatman (W1) and Rayon (R1, R2) filters indicated; **(c)** deployment at the Cape Verde sampling tower.

**Trace elements at
Cape Verde**
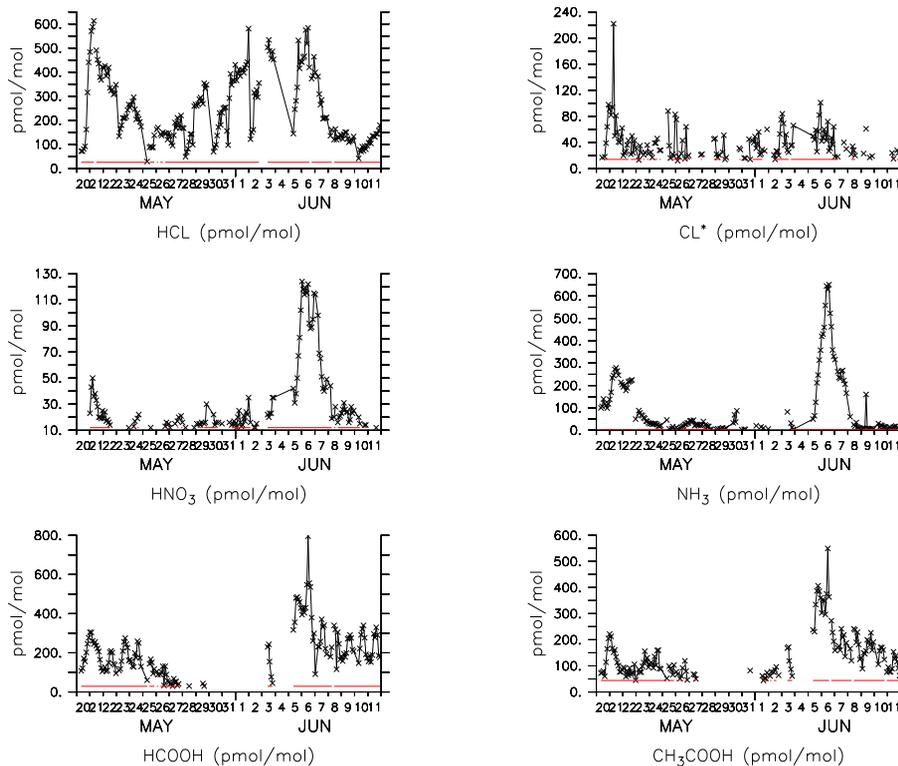
R. Sander et al.

**Fig. 6.** Time series of the mist chamber data. Clstar denotes reactive chlorine (Cl*). The red lines denote the detection limit.
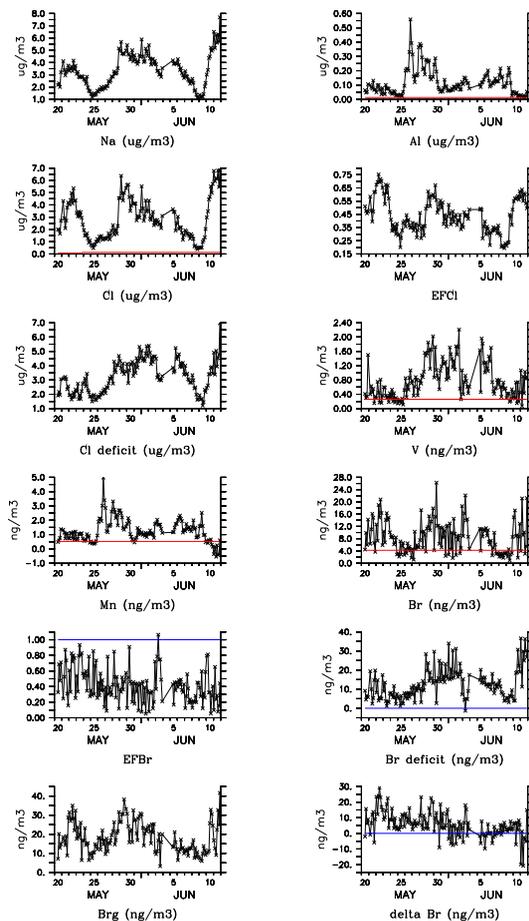
**Fig. 7.** Time series of the filter pack data, analyzed by NAA. The red lines denote the detection limit and the blue lines denote sea water composition, i.e., EF = 1 and deficit = 0.
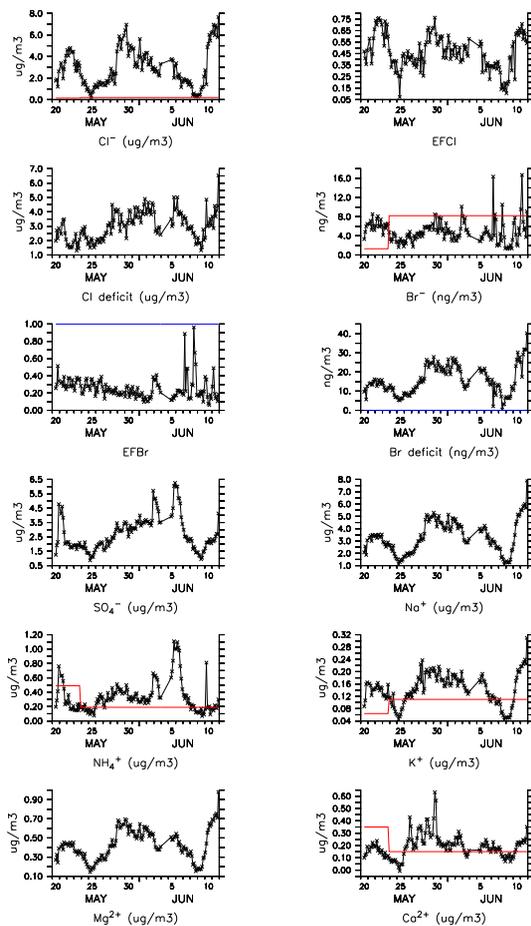
**Fig. 8.** Time series of the filter pack data, analyzed by IC. The red lines denote the detection limit and the blue lines denote sea water composition, i.e., EF = 1 and deficit = 0.
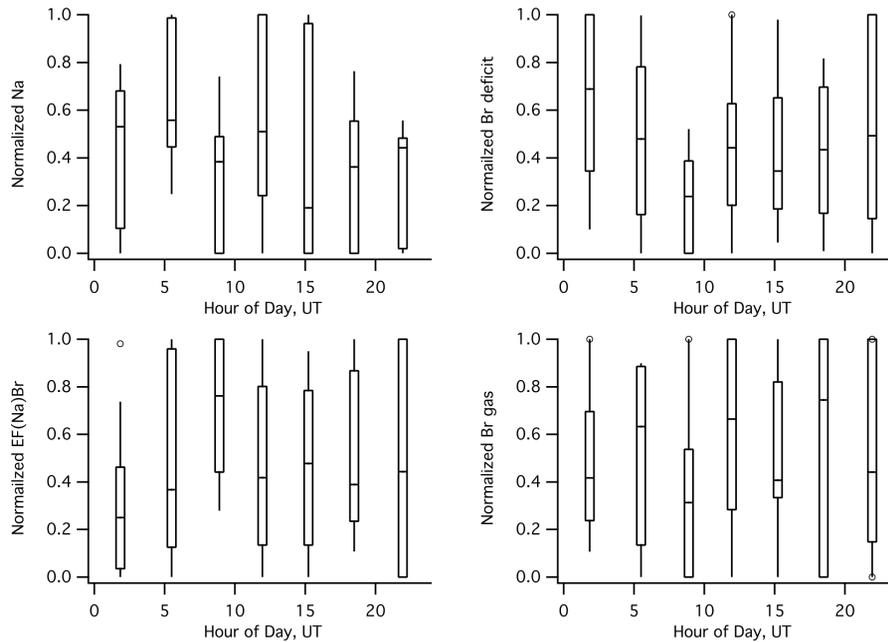
**Fig. 9.** Diel variability of normalized Na and Br data.
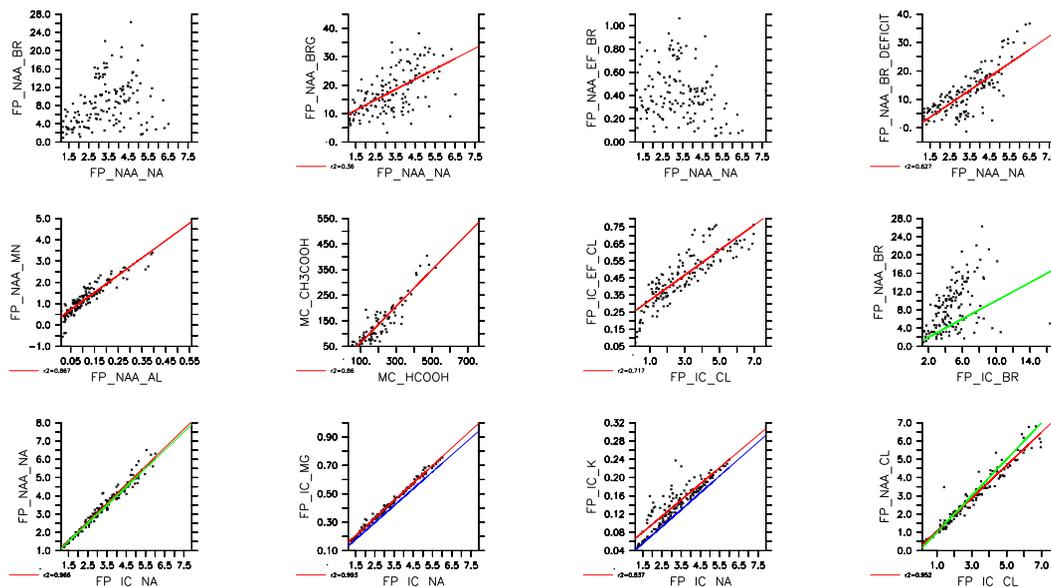
**Trace elements at Cape Verde**

R. Sander et al.



**Fig. 10.** Scatter plots. The prefixes FP_NAA and FP_IC denote filter pack samples analyzed by NAA and IC, respectively. The prefix MC refers to the mist chamber data. The units are the same as listed in Table 1. Regression lines in red are only shown if $r^2 > 0.3$. For the NAA vs. IC comparisons, a 1 : 1 line is shown in green. Blue lines refer to sea water composition.